MCF2L-AS1/miR-874-3p/STAT3 feedback loop contributes to lung adenocarcinoma cell growth and cisplatin resistance

Min Xu [a,1], Jing Zheng [b,1], Jun Wang [c], Haitao Huang [a], Gang Hu [a], Hailan He [d,*]

[a] Department of Respiratory and Critical Care Medicine, the Fifth People's Hospital of Chengdu, China
[b] Chengdu Women's and Children's Central Hospital, China
[c] Department of Hepatobiliary Surgery, the Fifth People's Hospital of Chengdu, China
[d] Department of Pediatrics, Sichuan Provincial People's Hospital, China

A B S T R A C T

Background: Long noncoding RNA (lncRNA) is widely acknowledged for its crucial role in the biological processes of various human cancers. MCF2L antisense RNA 1 (MCF2L-AS1) is a newly identified lncRNA, which remains unexplored in the context of cancer.
Methods: MCF2L-AS1 expression was examined using qRT-PCR analysis. The impact of MCF2L-AS1 on LUAD cell growth was assessed through CCK-8, colony formation, EdU, caspase-3 activity, TUNEL, Western blot, and transwell assays. The interaction between miR-874-3p and MCF2L-AS1 or STAT3 was confirmed by RIP, luciferase reporter, and RNA pull-down assays.
Results: Our study demonstrated the overexpression of MCF2L-AS1 in LUAD cells. Functionally, the silencing of MCF2L-AS1 hindered cell proliferation, migration, and invasion, while promoting cell apoptosis. Notably, the depletion of MCF2L-AS1 was associated with decreased cisplatin resistance. Mechanistically, MCF2L-AS1 was identified as an upstream gene of miR-874-3p, negatively regulating its expression. Following this, STAT3, the downstream target of miR-874-3p, was identified. Additionally, the expression of STAT3 was inversely related to miR-874-3p and positively regulated by MCF2L-AS1. A restoration assay suggested that MCF2L-AS1 promoted LUAD cell growth by sponging miR-874-3p and modulating STAT3 expression. Intriguingly, STAT3 was subsequently confirmed as a transcription factor that binds to the MCF2L-AS1 promoter, thereby enhancing its transcription.
Conclusions: The MCF2L-AS1/miR-874-3p/STAT3 feedback loop plays a significant role in LUAD cell growth and cisplatin resistance.

1. Background

Lung cancer, a prevalent type of malignancy, is a leading cause of death worldwide [1,2]. Extensive research suggests that lung cancer can be categorized into various subtypes, among which non-small cell lung cancer (NSCLC) is the most common, accounting for approximately 85 %. Moreover, based on histologic features, adenocarcinoma is recognized as the predominant subtype of NSCLC [3, 4]. Despite advancements in medical capabilities leading to significant progress in diagnostic and therapeutic strategies, the long-term survival rate for patients with malignant lung adenocarcinoma (LUAD) remains unsatisfactory [5]. Although LUAD exhibits relatively

high sensitivity to primary chemotherapy, the risk of mortality persists due to extensive regional metastasis and rapid development of chemoresistance [6,7]. Chemoresistance poses a significant challenge for patients diagnosed with LUAD during chemotherapy. Consequently, our focus is on enhancing the sensitivity of LUAD cells to cisplatin.

Long noncoding RNAs (lncRNAs) are transcripts exceeding 200 nucleotides in length with limited protein-coding capacity [8]. They can play either oncogenic or anti-carcinogenic roles in cancers, and their abnormal expression can initiate tumor formation [9, 10]. Initially, lncRNAs were considered "noise" of genomic transcription, a by-product of RNA polymerase II transcription, with no biological function. However, a 1991 report on X chromosome inactivation regulated by Xist challenged this view [11]. A subsequent 2007 report titled "Functional demarcation of active and silent chromatin domains in human HOX loci by noncoding RNAs" officially ushered in the era of lncRNAs. The continuous development of high-throughput sequencing in recent years has led to the identification of an increasing number of lncRNAs and their essential roles in various life processes such as epigenetic regulation, cell cycle regulation, and cell differentiation have been revealed [12]. Numerous reports have demonstrated that lncRNAs regulate gene expression through chromatin modification, transcription, and post-transcription regulation [13], impacting the onset of different types of tumors, including gastric cancer [14], cervical cancer [15], colorectal cancer [16], and others. As a result, certain differentially expressed lncRNAs have been identified as potential prognostic biomarkers for cancer patients [17]. Among them, lncRNAs can isolate their inhibitory effect on target genes by sponging miRNAs, thus playing a crucial role in the competitive endogenous RNA (ceRNA) network, which influences cancer progression [18]. Over the past few years, various lncRNAs have been reported to function as ceRNAs, indirectly mediating gene expression in LUAD progression [19–21].

Our study uncovered the oncogenic property of MCF2L-AS1 in LUAD and identified the MCF2L-AS1/miR-874-3p/STAT3 feedback loop's contribution to LUAD cell growth and cisplatin resistance. These findings could prove beneficial for the diagnosis and treatment of LUAD patients.

2. Methods

2.1. Cell culture

The human normal lung epithelial cell line, BEAS-2B, along with lung adenocarcinoma (LUAD) cell lines such as HCC827, A549, and NCI–H23, were acquired from the American Type Culture Collection (ATCC, Manassas, VA, USA). In addition, the LUAD cell line PC9 was sourced from Procell Life Science & Technology (Wuhan, China). These cell lines were cultured in RPMI 1640 medium, supplied by Thermo Fisher Scientific (Waltham, MA, USA), and maintained in an incubator at 37 °C with a 5 % CO_2 atmosphere. Antibiotics (penicillin, streptomycin) and 10 % fetal bovine serum (FBS) were bought from Invitrogen (Carlsbad, CA, USA) and added to the culture medium.

2.2. Total RNA extraction and qRT-PCR

Total cellular RNAs of PC9 and A549 cells were acquired by TRIzol reagent (Invitrogen) following the standard method. Reverse transcription was achieved using 1 μg of total RNA and SuperScript RT (Fermentas, Ottawa, Canada). Quantitative PCR was conducted with SYBR Green PCR kit (Takara, Otsu, Japan) on StepOne Real-Time PCR System (Thermo Fisher Scientific). Gene expression was calculated by the comparative threshold cycle (Ct) method and normalized to U6 or GAPDH.

2.3. Cell transfection

The MCF2L-AS1 or STAT3-specific shRNAs (sh-MCF2L-AS1#1/2, sh-STAT3#1/2) and control (sh-NC), the pcDNA3.1/STAT3 and control (pcDNA3.1) were procured from Genepharma (Shanghai, China) for plasmid transfection. The miR-874-3p mimics/inhibitor and NC mimics/inhibitor were also from Genepharma. PC9 and A549 cells in 24-well plates were cultured to about 80 % confluence for transfecting with indicated plasmids using Lipofectamine 2000 (Invitrogen). 48 h later, cells were reaped for subsequent assays.

2.4. Cell counting kit-8 (CCK-8)

2×10^3 LUAD cells in 96-well plates were mixed with 10 μl of CCK8 (Solarbio, Beijing, China) for 2 h in 5 % CO_2 at 37 °C. The absorbance at 450 nm of each sample was monitored at 0, 24, 43, 72, 96 h after treatment.

2.5. Colony formation

5×10^2 LUAD cells were planted in 6-well plates for 14 days, with culture medium was changed every 3 days. Visible colonies were stained by crystal violet (Beyotime, Shanghai, China) and counted after fixation.

2.6. EdU assay

The BeyoClick™ EdU Cell Proliferation Kit with Alexa Fluor 488 was procured from Beyotime. LUAD cells were transfected for 48 h, then treated with EdU medium diluent and Hoechst 33342 (Beyotime). Images of stained cells were taken by fluorescent microscope (Leica, Wetzlar, Germany).

2.7. Caspase-3 assay

The Beyotime C1115 Caspase 3 Activity Assay Kit was procured for determining caspase-3 activity in cell lysates of PC9 and A549 as per the guidebook. The extracted protein samples in 96-well plates were cultivated with the reaction buffer in the presence of caspase substrate for 4 h. The complex was finally monitored by microplate reader (Tecan, Männedorf, Switzerland) at wavelength of 405 nm.

2.8. TUNEL assay

The transfected LUAD cells in 1 % formaldehyde were first treated with 0.2 % Triton X-100, then with dUTP-end labeling kit (Clontech, Mountain View, CA, USA). Apoptotic cells were assessed by fluorescence microscope after staining with DAPI (Beyotime).

2.9. Western blotting

The equal amount of protein sample was separated on 10 % SDs-PAGE and transferred to polyvinylidene difluoride (PVDF) membranes. Following blocking by 5 % nonfat milk, samples on membranes were subjected to the specific primary antibodies (Abcam, Cambridge, MA, USA) against MMP2, MMP9, GAPDH and STAT3 all night. Samples were then washed and incubated with anti-IgG secondary antibody. Protein bands were analyzed by ECL chemiluminescence Detection kit (Millipore, Billerica, MA, USA).

2.10. Cell invasion assay

The Matrigel-coated transwell inserts were purchased from Corning (Corning, NY, USA) for invasion assay. 5×10^3 cells were cultured in serum-free culture medium and seeded to the upper chamber, while the conditioned medium was put into the lower chamber. Invasive cells were mixed with 4 % paraformaldehyde, then with crystal violet, followed by the observation under microscope (Thermo Fisher Scientific).

2.11. MTT assay

Cisplatin-resistance was detected in PC9 and A549 cells by MTT (Sigma-Aldrich, St. Louis, MI, USA). Cells in 96-well plates (1×10^4 cells/well) were treated with varied concentrations of cisplatin (Sigma-Aldrich) at 37 °C in 5 % CO_2 for 48 h, then with 5 mg/ml of MTT in phosphate buffered saline (PBS). After removing culture medium, the crystal was solubilized by 150 μl of DMSO (Sigma-Aldrich). Cell viability was determined by analyzing the absorbance at 490 nm.

2.12. Nucleus-cytoplasm separation

Isolation of nuclear and cytoplasmic RNAs was achieved in PC9 and A549 cells by use of PARIS™ Kit (Invitrogen). Lysed cells in cell fraction buffer were centrifuged, and the supernatant (cell cytoplasm) was collected. The cell disruption buffer was then added for lysing cell nuclei. At last, qRT-PCR was conducted for MCF2L-AS1, U6 or GAPDH.

3. FISH

The FISH was carried out in LUAD cells for determining the localization of MCF2L-AS1 using the specific RNA FISH probe (RiboBio). After nucleus was counterstained with Hoechst, stained cells were analyzed by laser scanning confocal microscope (ZEISS, Jena, Germany).

3.1. RNA immunoprecipitation (RIP)

Magna RNA-binding protein immunoprecipitation kit was obtained from Millipore for RIP assay. Lysates were cultivated in RIP buffer adding magnetic beads conjugated to human anti-Ago2 or IgG antibody (Millipore). The precipitated RNAs were purified and extracted for qRT-PCR.

3.2. Dual-luciferase reporter gene analysis

The wild-type (WT) and mutant (Mut) MCF2L-AS1 sequence or STAT3 3′-UTR to miR-874-3p binding sites were used for inserting to the pmirGLO luciferase vector (Promega, Madison, WI, USA). The reporter vectors MCF2L-AS1-WT/Mut and STAT3-WT/Mut were generated and co-transfected with miR-874-3p mimics and NC mimics into cells. For promoter analysis, the MCF2L-AS1 promoter binding sites to STAT3-WT or Mut were integrated into pGL3 promoter vector (Promega) to form promoter-WT/Mut constructs. Then, promoter constructs were co-transfected with sh-STAT3 and sh-NC or pcDNA3.1/STAT3 and pcDNA3.1 to cells. 48 h later, dual-luciferase reporter assay kit (Promega) was finally employed.
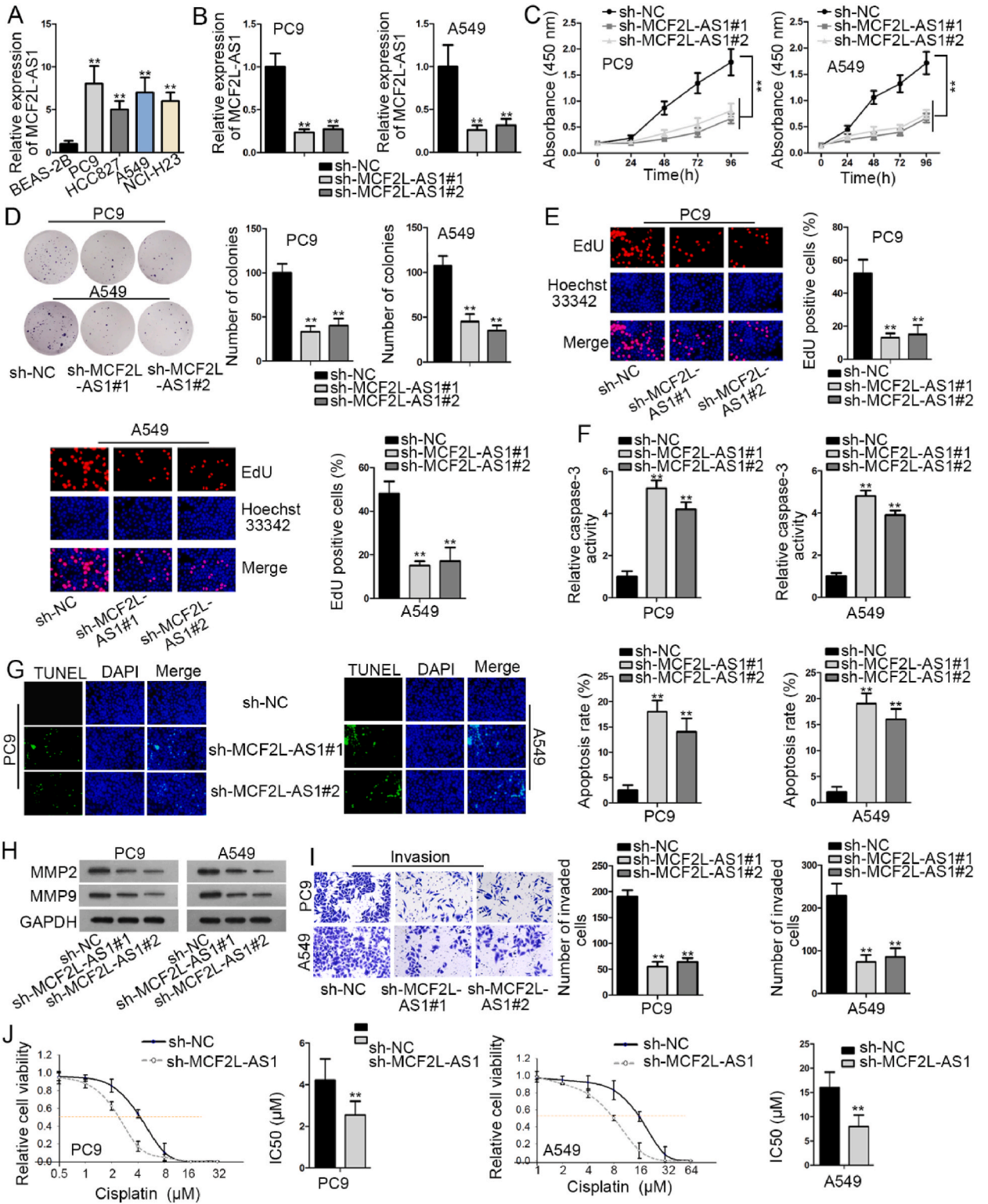
(caption on next page)

Fig. 1. Upregulated MCF2L-AS1 promotes LUAD cell growth and cisplatin resistance. (A) The expression level of MCF2L-AS1 in human normal lung epithelial cell line (BEAS-2B) and LUAD cell lines (PC9, HCC827, A549 and NCI–H23). (B) The knockdown efficiency of sh-MCF2L-AS1#1/2 in LIAD cells. (C–E) Cell proliferation was evaluated in sh-MCF2L-AS1 transfected cells by performing CCK-8, colony formation and EdU assays. (F–G) Caspase-3 activity assay and TUNEL assay were carried out to examine cell apoptosis in LUAD MCF2L-AS1 silenced LUAD cells. (H) The migration of LUAD cells was tested with Western blot assay upon MCF2L-AS1 depletion. (I) Transwell assay was conducted to assess the invasion in LUAD cells transfected with sh-MCF2L-AS1. (J) The effect of MCF2L-AS1 knockdown on cell viability in cisplatin treated LUAD cells was measured with MTT assay. **P < 0.01.

3.3. RNA pull-down assay

Pierce Magnetic RNA-Protein Pull-Down Kit was acquired from Thermo Fisher Scientific for RNA pull-down assay in LUAD cells utilizing the biotinylated RNAs (miR-874-3p biotin probe), with miR-874-3p no-biotin probe as control. After adding magnetic beads, the complex was analyzed using qRT-PCR.

3.4. Chromatin immunoprecipitation (ChIP)

The crosslinked chromatin was sonicated to chromatin fragments of 200-500-bp, then immunoprecipitated with antibody against STAT3 or IgG (Millipore). Precipitates were examined by qRT-PCR.

3.5. Statistical analysis

Data were statistically analyzed via *t*-test or ANOVA (one-way) utilizing PRISM 6 (GraphPad, San Diego, CA, USA), and expressed as mean $\pm$ SD. The significant level was set as p < 0.05.

4. Results

4.1. Upregulated MCF2L-AS1 promotes LUAD cell growth and cisplatin resistance

Firstly, MCF2L-AS1 expression was measured in the human normal lung epithelial cell line (BEAS-2B) and LUAD cell lines (PC9, HCC827, A549 and NCI–H23). Consequently, MCF2L-AS1 expression was significantly higher in the LUAD cell lines compared to BEAS-2B cells (Fig. 1A). Due to their relatively higher expression, PC9 and A549 cells were selected for subsequent assays. To investigate the biological function of MCF2L-AS1 in LUAD, loss-of-function experiments were designed and implemented. Prior to the experiments, specific MCF2L-AS1 shRNAs (sh-MCF2L-AS1#1 and sh-MCF2L-AS1#2) were transfected into PC9 and A549 cells. The results illustrated that MCF2L-AS1 expression was markedly decreased upon upon transfection with sh-MCF2L-AS1#1/2 (Fig. 1B). Hence, these two plasmids were utilized for the loss-of-function experiments. CCK-8 and colony formation assays were conducted to examine the proliferative ability of PC9 and A549 cells. It was observed that MCF2L-AS1 knockdown led to reduced cell proliferation (Fig. 1C–D). EdU assay further validated the inhibitory effect of silenced MCF2L-AS1 on the proliferation of PC9 and A549 cells (Fig. 1E). Additionally, cell apoptosis was evaluated by performing caspase-3 activity and TUNEL assays. Intriguingly, apoptosis was remarkably enhanced in sh-MCF2L-AS1 transfected PC9 and A549 cells (Fig. 1F–G). Through Western blot analysis, decreased levels of migration-associated proteins (MMP2 and MMP9) were detected following MCF2L-AS1 depletion (Fig. 1H). Moreover, the transwell assay indicated that cell invasion was more suppressed in the sh-MCF2L-AS1 group compared to the sh-NC group (Fig. 1I). We next sought to investigate the function of MCF2L-AS1 on cisplatin resistance. Cisplatin was introduced to PC9 and A549 cells. Post-treatment, the IC50 value was determined by MTT assay. As hypothesized, transfection of sh-MCF2L-AS1 reduced the IC50 value of PC9 and A549 cells (Fig. 1J). In summary, upregulated MCF2L-AS1 promotes LUAD cell growth and cisplatin resistance.

4.2. MCF2L-AS1 sponges miR-874-3p in LUAD

To elucidate the molecular mechanism of MCF2L-AS1, we first determined its subcellular distribution in LUAD cells. Through subcellular fractionation and FISH assays, we found that MCF2L-AS1 was predominantly localized in the cytoplasm (Fig. 2A–B), providing evidence for the ceRNA hypothesis. Next, starBase 3.0 (http://starbase.sysu.edu.cn/) predicted 7 miRNAs that could potentially bind to MCF2L-AS1 (Fig. 2C). qRT-PCR analysis was utilized to examine the expression of these candidate miRNAs in LUAD cells. Among them, miR-874-3p exhibited the highest fold change (Fig. 2D), and was found to be expressed at low levels in LUAD cells (Fig. 2E). Moreover, miR-874-3p expression was markedly upregulated following MCF2L-AS1 knockdown (Fig. 2F). Ago2 (Argonaute 2) is the sole AGO family member with catalytic activity, functioning as a key component of the RNA-induced silencing complex (RISC) and a critical regulator of miRNA activity [22]. Fig. 2G showed that both MCF2L-AS1 and miR-874-3p were present in the Ago2 immunoprecipitate, indicating a potential interaction between MCF2L-AS1 and miR-874-3p. Subsequently, the MCF2L-AS1 sequence was predicted to contain a binding site for miR-874-3p (Fig. 2H). To investigate whether MCF2L-AS1 sponges miR-874-3p, we elevated miR-874-3p expression by transfecting miR-874-3p mimics into LUAD cells (Fig. 2I), and performed a luciferase reporter assay in PC9 and A549 cells. MCF2L-AS1-WT and MCF2L-AS1-Mut constructs were co-transfected with either NC mimics or miR-874-3p mimics. The results demonstrated that miR-874-3p overexpression markedly reduced the luciferase activity of the MCF2L-AS1-WT reporter but not the MCF2L-AS1-Mut reporter, indicating direct binding between MCF2L-AS1 and miR-874-3p (Fig. 2J). Taken together, these data
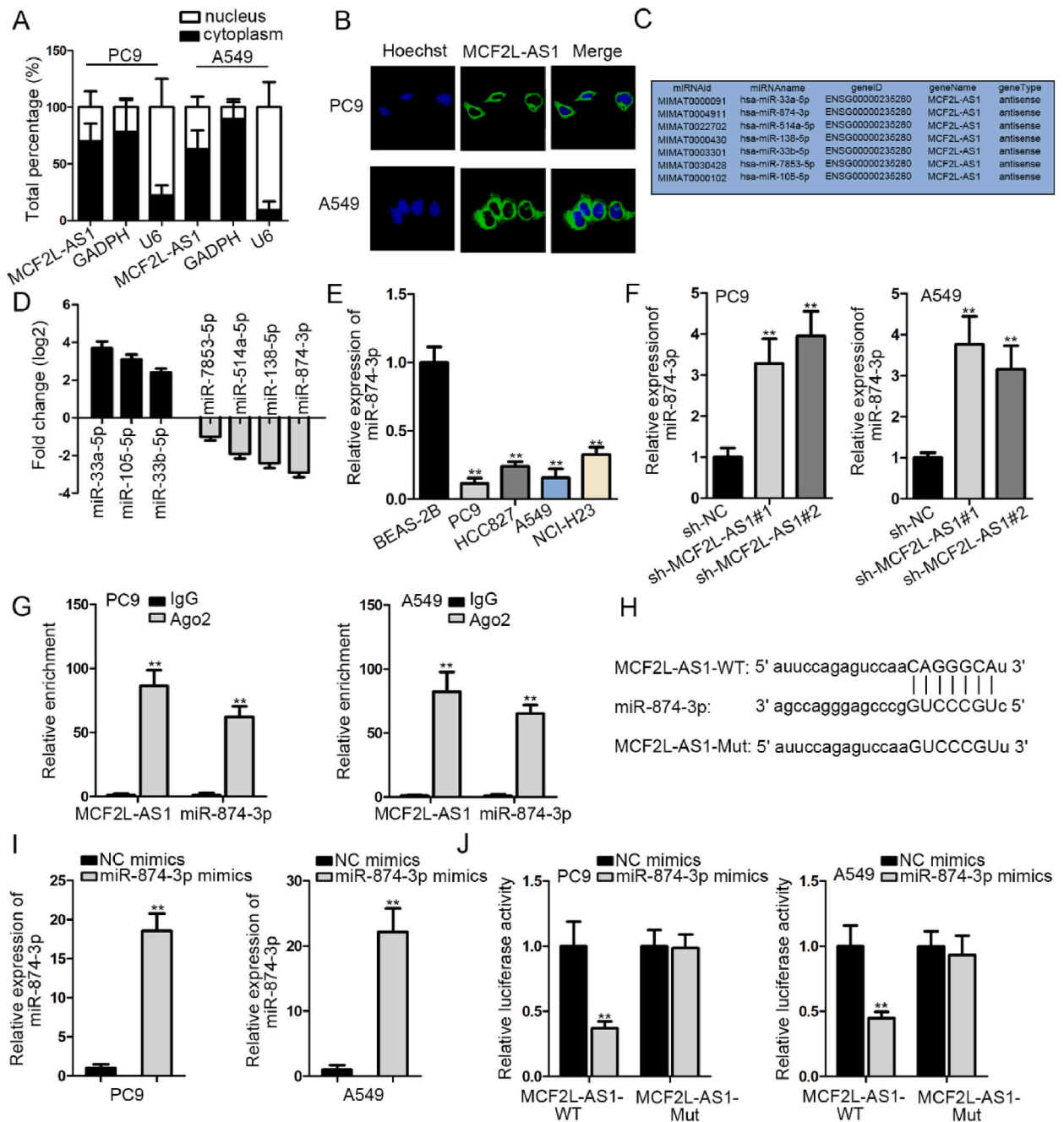
Fig. 2. MCF2L-AS1 sponges miR-874-3p in LUAD. (A–B) Subcellular fractionation and FISH assays were used to determine the distribution of MCF2L-AS1 in LUAD cells. (C) The predicted miRNAs for MCF2L-AS1 from starBase. (D) The expressions of potential miRNAs in LUAD cells. (E) MiR-874-3p expression in human normal lung epithelial cell line (BEAS-2B) and LUAD cell lines (PC9, HCC827, A549 and NCI–H23). (F) The expression level of miR-874-3p in sh-MCF2L-AS1 transfected cells. (G) RIP assay was applied to evaluate the interaction between MCF2L-AS1 and miR-874-3p. (H) The binding site between MCF2L-AS1 and miR-874-3p. (I) Transfection efficiency of miR-874-3p mimics was tested in LUAD cells. (J) Luciferase reporter assay was employed to further confirm the combination of miR-874-3p in MCF2L-AS1. $**P < 0.01$.

suggest that MCF2L-AS1 acts as a sponge for miR-874-3p in LUAD.

4.3. STAT3 is a target of miR-874-3p

To identify the downstream target of miR-874-3p in LUAD, we searched the PITA, PicTar, miRanda, microT and miRmap databases to predict potential mRNA targets of miR-874-3p. The results revealed 27 mRNAs that could be targeted by miR-874-3p (Fig. 3A).
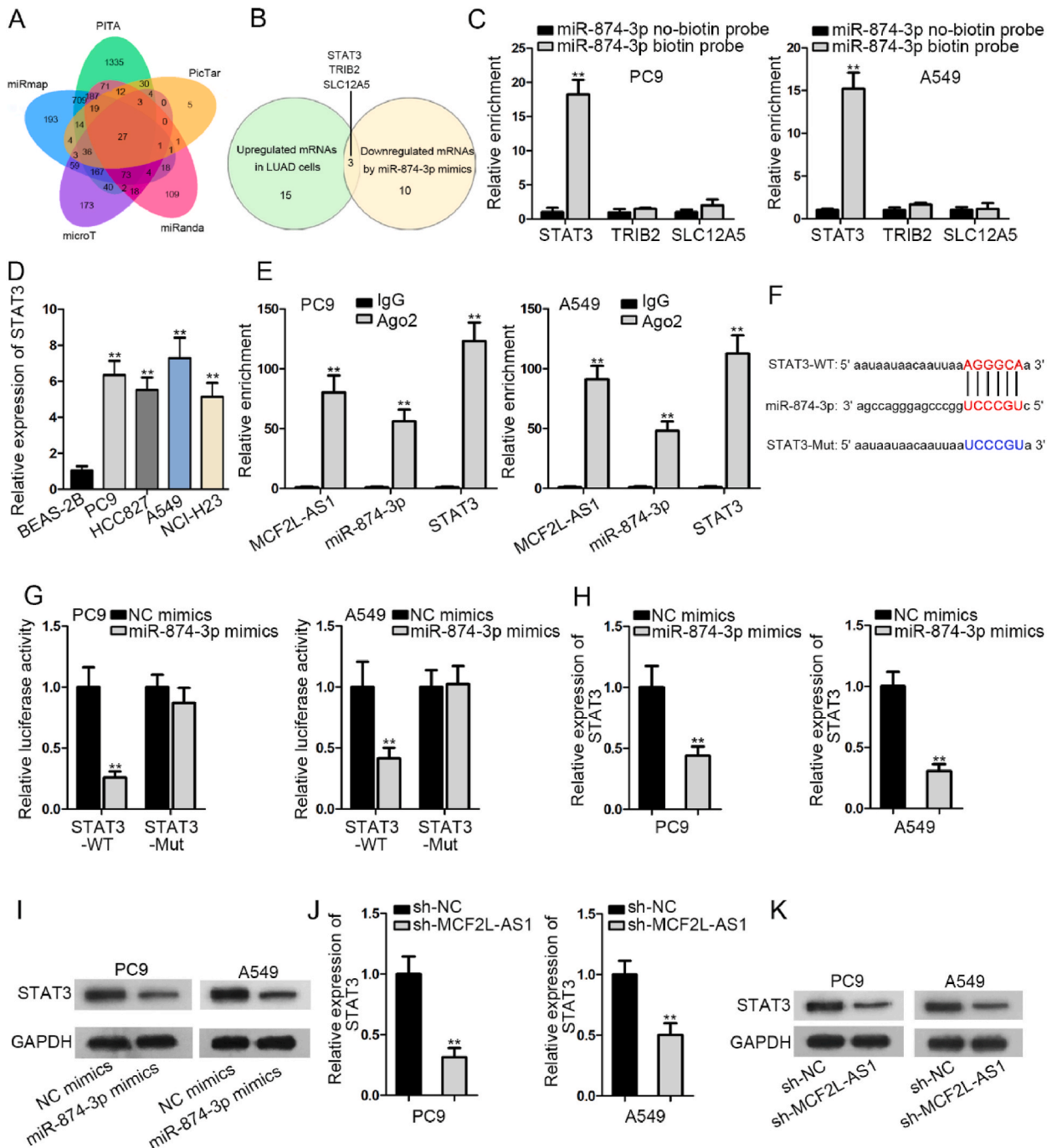
Fig. 3. STAT3 is a target of miR-874-3p. (A) Potential target mRNAs of miR-874-3p predicted by PITA, PicTar, miRanda, microT and miRmap. (B) Underlying downstream mRNAs that could be upregulated in LUAD cells and downregulated by miR-874-3p mimics. (C) RNA pull-down assay was utilized to examine the enrichment of STAT3, TRIB2 and SLC12A5 in miR-874-3p biotin probe. (D) The expression of STAT3 in human normal lung epithelial cell line (BEAS-2B) and LUAD cell lines (PC9, HCC827, A549 and NCI–H23). (E) The interaction between miR-874-3p together with MCF2L-AS1 and STAT3 was determined by RIP assay. (F) The potential binding site between miR-874-3p and STAT3 was predicted through starBase. (G) MiR-874-3p was verified to combine with STAT3 through luciferase reporter assay. (H–I) STAT3 mRNA and protein levels were assessed in LUAD cells transfected with miR-874-3p mimics. (J–K) qRT-PCR and Western blot assays were employed to detect the mRNA and protein levels of STAT3 in MCF2L-AS1 downregulated LUAD cells. **P < 0.01.
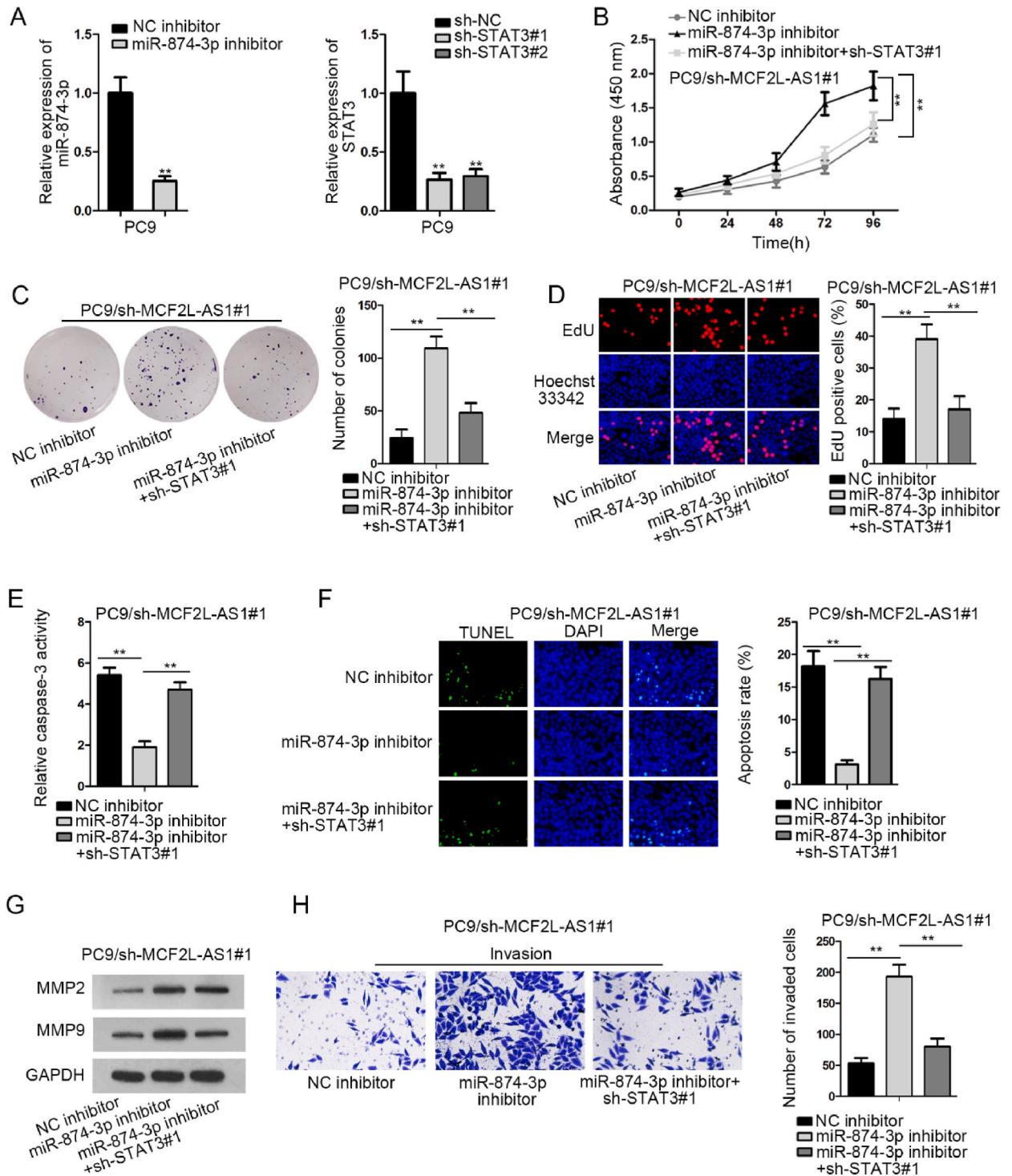
Fig. 4. MCF2L-AS1 facilitate LUAD cell growth by targeting miR-874-3p/STAT3. (A) Expressions of miR-874-3p and STAT3 were tested by separately transfecting miR-874-3p inhibitor and sh-STAT3. (B–D) The proliferative capacity of MCF2L-AS1 silenced cells was estimated after transfecting NC inhibitor, miR-874-3p inhibitor, miR-874-3p inhibitor plus sh-STAT3. (E–F) NC inhibitor, miR-874-3p inhibitor, miR-874-3p inhibitor plus sh-STAT3 were transfected into MCF2L-AS1 downregulated cells to observe cell apoptosis. (G) Cell migration was evaluated after transfecting above appointed plasmids in sh-MCF2L-AS1 transfected cells. (H) Above appointed plasmids were transfected into MCF2L-AS1 downregulated cells to detect cell invasion. **P < 0.01.
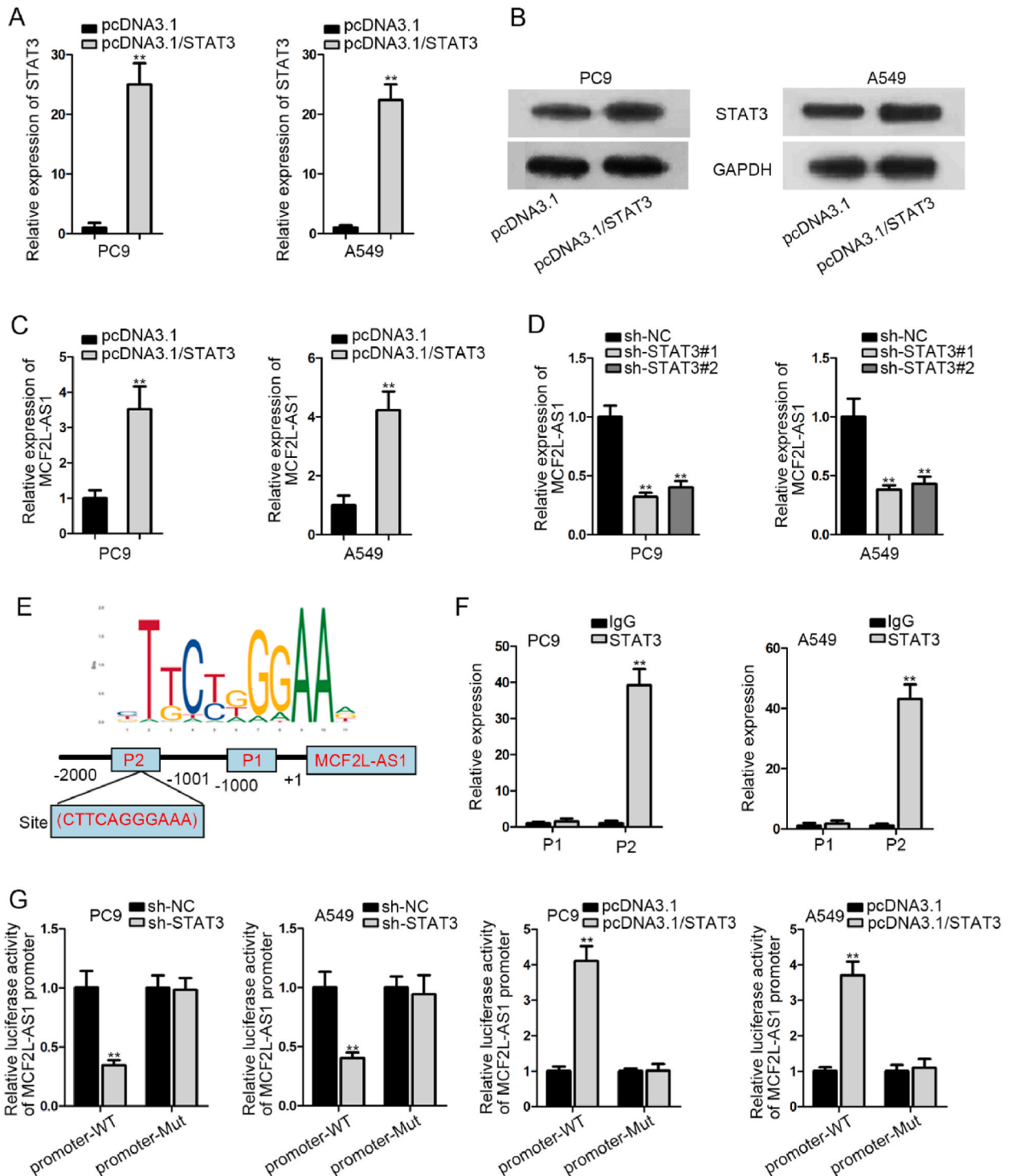
Fig. 5. STAT3 binds to MCF2L-AS1 promoter. (A–B) The overexpression efficiency of STAT3 was detected in LUAD cells. (C) MCF2L-AS1 expression in STAT3 overexpressed LUAD cells. (D) The effect of STAT3 knockdown on MCF2L-AS1 expression. (E) The binding sites between STAT3 and MCF2L-AS1 promoter. (F) ChIP assay was performed to determine the interaction between STAT3 and MCF2L-AS1 promoter. (G) Luciferase reporter assay was utilized to measure the combination of STAT3 in MCF2L-AS1 promoter. **P < 0.01.

Subsequently, 15 upregulated mRNAs were identified in LUAD cells, of which 10 were downregulated by miR-874-3p mimics. Among them, STAT3, TRIB2 and SLC12A5 were selected for further analysis (Fig. 3B). To confirm the bona fide target of miR-874-3p, an RNA pull-down assay was performed. STAT3 was found to be substantially enriched in the miR-874-3p biotin probe compared to TRIB2 and SLC12A5 (Fig. 3C), suggesting STAT3 could be a downstream target of miR-874-3p. Consistently, STAT3 was highly expressed in LUAD cells (Fig. 3D). RIP assay results demonstrated the presence of miR-874-3p, MCF2L-AS1 and STAT3 in the Ago2 immunoprecipitate, indicating that MCF2L-AS1 and STAT3 interact with the RISC complex formed by miR-874-3p and Ago2 (Fig. 3E). Using starBase 3.0, a miR-874-3p binding site was identified in the STAT3 3′-UTR (Fig. 3F). Subsequently, a luciferase reporter assay was conducted using a luciferase plasmid carrying the STAT3 3′-UTR sequence containing the predicted miR-874-3p binding sites. A mutant STAT3 reporter was also generated. These plasmids were introduced into PC9 and A549 cells along with miR-874-3p mimics. The results showed that miR-874-3p mimics decreased luciferase activity in cells transfected with wild-type STAT3 but not mutant STAT3 (Fig. 3G). This demonstrated that STAT3 can sequester miR-874-3p, indicating direct binding of miR-874-3p to the STAT3 3′-UTR. Additionally, miR-874-3p mimics were found to inhibit STAT3 mRNA and protein levels (Fig. 3H–I). Similarly, STAT3 mRNA and protein expression was reduced upon MCF2L-AS1 knockdown (Fig. 3J–K). In summary, these data confirm STAT3 as a direct target of miR-874-3p.

4.4. MCF2L-AS1 facilitates LUAD cell growth by targeting miR-874-3p/STAT3

To further elucidate the MCF2L-AS1/miR-874-3p/STAT3 axis in LUAD, restoration assays were conducted. The expression of miR-874-3p and STAT3 were decreased by separately transfecting miR-874-3p inhibitor and sh-STAT3 (Fig. 4A). CCK-8 and colony formation assays displayed that STAT3 knockdown counteracted the promotive effect of miR-874-3p inhibition on cell proliferation in MCF2L-AS1 downregulated LUAD cells (Fig. 4B–C), consistent with the results of the EdU assay (Fig. 4D). Next, cell apoptosis was evaluated by caspase-3 activity and TUNEL assays. The results showed that apoptosis inhibition by miR-874-3p inhibitor was rescued by silenced STAT3 in sh-MCF2L-AS1 transfected cells (Fig. 4E–F). Subsequently, Western blot and transwell assays were conducted to examine cell migration and invasion. As shown in Fig. 4G, miR-874-3p repression enhanced the migratory capacity of LUAD cells, while co-transfection of sh-STAT3 countervailed this promotive effect in sh-MCF2L-AS1 transfected cells. Similarly, the enhanced invasion caused by miR-874-3p inhibitor in LUAD cells was abrogated by sh-STAT3 transfection in MCF2L-AS1-silenced cells (Fig. 4H). In summary, these results demonstrate that MCF2L-AS1 facilitates LUAD cell growth by regulating the miR-874-3p/STAT3 axis.

4.5. STAT3 binds to MCF2L-AS1 promoter

It has been reported that STAT3 can function as a transcription factor to activate lncRNA transcription by interacting with lncRNA promoters [23]. To investigate whether STAT3 exerts this function in LUAD, a series of experiments were conducted. Firstly, the overexpression efficiency of STAT3 was detected. The results showed that STAT3 mRNA and protein levels were significantly upregulated upon transfection with pcDNA3.1/STAT3 (Fig. 5A–B). Subsequently, we found that MCF2L-AS1 expression was increased in pcDNA3.1/STAT3 transfected LUAD cells (Fig. 5C). Furthermore, its expression was downregulated following STAT3 knockdown (Fig. 5D). These results revealed a positive correlation between STAT3 and MCF2L-AS1. Through JASPAR (http://jaspar.genereg.net/), STAT3 was predicted to have a binding sequence in the MCF2L-AS1 promoter, containing two potential binding sites (P1 and P2) (Fig. 5E). ChIP analysis further showed stronger binding at the P2 site, indicating that STAT3 could directly bind to the MCF2L-AS1 promoter (Fig. 5F). Luciferase reporter assay revealed that the luciferase activity of the wild-type MCF2L-AS1 promoter was decreased by sh-STAT3 and increased with pcDNA3.1/STAT3, but no significant change was observed with the mutant MCF2L-AS1 promoter (Fig. 5G). Taken together, these results demonstrate that STAT3 can enhance MCF2L-AS1 expression by directly binding to its promoter region.

5. Discussion

LncRNAs have been suggested to play important regulatory roles in cancer cell proliferation, differentiation, and apoptosis [24,25]. Importantly, aberrantly expressed lncRNAs are also well-known for their crucial functions in initiating and driving cancer progression. For example, the downregulated lncRNA lnc-GNAT1-1 acts as a tumor suppressor in colorectal cancer by modulating the RKIP–NF–κB-Snail circuit [26]. The lncRNA BANCR is downregulated in bladder cancer and inhibits its malignant phenotypes [27]. The lncRNA MALAT1 promotes hepatocellular carcinoma development by upregulating SRSF1 and activating mTOR [28]. Substantial evidence has shown that chemoresistance leads to poor therapeutic outcomes for LUAD patients. Aberrant lncRNA expression has been widely implicated as a key driver of chemoresistance [29], underscoring the need to elucidate the underlying mechanisms. In this study, we found high expression of MCF2L-AS1 in LUAD cells. Silencing of MCF2L-AS1 was associated with inhibited proliferation, migration, invasion, cisplatin resistance, and promoted apoptosis. These results suggest MCF2L-AS1 acts as an oncogene in LUAD and contributes to cisplatin resistance.

The ceRNA network comprising lncRNA-miRNA-mRNA crosstalk has been described in human cancers. In this network, lncRNAs regulate post-transcriptional gene expression by sequestering miRNAs to upregulate mRNA targets [30,31]. MiRNAs are short 22–24 nucleotide RNAs that play important regulatory roles in cancer progression [32–34]. For example, miRNA-204-5p regulates breast cancer cell growth and metastasis [35], while miRNA-7 acts as a tumor suppressor and potential therapeutic target in gastric cancer [36]. In the ceRNA network, the lncRNA LINC00346 sponges miR-188-3p to promote tumor growth and gemcitabine resistance in pancreatic cancer by regulating BRD4 [37]. CeRNA networks are also widely reported in LUAD, including the SNHG6/miR-26a-5p/E2F7 axis that promotes cell cycle progression and proliferation [38], and the lncRNA TTN-AS1 that sponges

miR-142-5p to regulate CDK5 and epithelial-mesenchymal transition [39]. Our study identified downregulated miR-874-3p in LUAD cells, which was confirmed to interact with MCF2L-AS1. These results depict MCF2L-AS1 as a sponge for miR-874-3p.

The transcription factor STAT3 is constitutively activated in many cancers, including LUAD [40]. STAT3 can bind to the promoter regions of target genes to initiate transcription [41]. For instance, STAT3-induced HNF1A-AS1 overexpression promotes oral squamous cell carcinoma proliferation and migration by activating Notch signaling [42]. STAT3-upregulation of LINC01287 regulates hepato-cellular carcinoma cell growth by sequestering miR-298 [43]. In gallbladder cancer, the STAT3-induced lncRNA HEGBC enhances tumorigenesis and metastasis. Our study demonstrated STAT3 is a target of miR-874-3p, with an inverse correlation between miR-874-3p and positive correlation with MCF2L-AS1 in LUAD cells. Further, we found STAT3 enhances MCF2L-AS1 promoter activity, forming a positive feedback loop between MCF2L-AS1 and STAT3.

6. Conclusions

In conclusion, this study demonstrated that MCF2L-AS1 is markedly overexpressed in LUAD. The MCF2L-AS1/miR-874-3p/STAT3 feedback loop contributes to LUAD cell growth and cisplatin resistance, providing valuable evidence to inform therapeutic strategies for LUAD patients.

Ethics statement

None.

CRediT authorship contribution statement

Min Xu: Data curation, Formal analysis, Investigation, Project administration, Resources, Software, Supervision, Validation, Visualization, Writing – original draft, Writing – review & editing. **Jing Zheng:** Investigation, Methodology, Software, Visualization, Writing – original draft, Writing – review & editing. **Jun Wang:** Investigation, Software, Writing – review & editing. **Haitao Huang:** Methodology, Supervision, Writing – original draft. **Gang Hu:** Data curation, Software, Writing – review & editing. **Hailan He:** Conceptualization, Project administration, Writing – original draft, Writing – review & editing.

Declaration of competing interest

The authors declare that they have no conflict of interest.

Acknowledgement

We appreciate the supports of laboratory technicians.

List of abbreviations

lncRNA   long noncoding RNA
LUAD   lung adenocarcinoma
MCF2L-AS1 MCF2L antisense RNA 1
STAT3   Signal transducer and activator of transcription 3
FBS   fetal bovine serum
qRT-PCR   quantitative real-time polymerase chain reaction
GAPDH   glyceraldehyde-3-phosphate dehydrogenase
shRNA   short hairpin RNA
NC   negative control
CCK-8   cell counting kit-8
PVDF   polyvinylidene fluoride
IgG   Immunoglobulin G
ChIP   Chromatin immunoprecipitation
SD   standard deviation
ceRNA   competing endogenous RNA
miRNAs   microRNAs

References

[1] M. Rahman, F. Shad, M.C. Smith, Acute kidney injury: a guide to diagnosis and management, Am. Fam. Physician 86 (7) (2012) 631–639.
[2] R. Siegel, et al., Cancer statistics, CA - Cancer J. Clin. 64 (1) (2014) 9–29, 2014.

[3] C. Allemani, et al., Global surveillance of cancer survival 1995-2009: analysis of individual data for 25,676,887 patients from 279 population-based registries in 67 countries (CONCORD-2), Lancet 385 (9972) (2015) 977–1010.

[4] L. Cheng, et al., Molecular pathology of lung cancer: key to personalized medicine, Mod. Pathol. 25 (3) (2012) 347–369.

[5] S.P. Riaz, et al., Trends in incidence of small cell lung cancer and all lung cancer, Lung Cancer 75 (3) (2012) 280–284.

[6] N. Murray, A.T. Turrisi 3rd, A review of first-line treatment for small-cell lung cancer, J. Thorac. Oncol. 1 (3) (2006) 270–278.

[7] S. Sarvi, et al., CD133+ cancer stem-like cells in small cell lung cancer are highly tumorigenic and chemoresistant but sensitive to a novel neuropeptide antagonist, Cancer Res. 74 (5) (2014) 1554–1565.

[8] K. Katsushima, et al., Targeting the Notch-regulated non-coding RNA TUG1 for glioma treatment, Nat. Commun. 7 (2016), 13616.

[9] X. Wang, et al., Long intragenic non-coding RNA lincRNA-p21 suppresses development of human prostate cancer, Cell Prolif. 50 (2) (2017).

[10] L. Chen, et al., Overexpression of LncRNA-UCA1 correlates with lung adenocarcinoma progression and poor prognosis, Clin. Lab. 65 (3) (2019).

[11] G. Borsani, et al., Characterization of a murine gene expressed from the inactive X chromosome, Nature 351 (6324) (1991) 325–329.

[12] W.X. Peng, P. Koirala, Y.Y. Mo, LncRNA-mediated regulation of cell signaling in cancer, Oncogene 36 (41) (2017) 5661–5667.

[13] T.R. Mercer, M.E. Dinger, J.S. Mattick, Long non-coding RNAs: insights into functions, Nat. Rev. Genet. 10 (3) (2009) 155–159.

[14] Y. Huang, et al., LncRNA AK023391 promotes tumorigenesis and invasion of gastric cancer through activation of the PI3K/Akt signaling pathway, J. Exp. Clin. Cancer Res. 36 (1) (2017) 194.

[15] C. Shang, et al., LNMICC promotes nodal metastasis of cervical cancer by reprogramming fatty acid metabolism, Cancer Res. 78 (4) (2018) 877–890.

[16] D.L. Chen, et al., Long non-coding RNA UICLM promotes colorectal cancer liver metastasis by acting as a ceRNA for microRNA-215 to regulate ZEB2 expression, Theranostics 7 (19) (2017) 4836–4849.

[17] B.S. Tan, et al., LncRNA NORAD is repressed by the YAP pathway and suppresses lung and breast cancer metastasis by sequestering S100P, Oncogene 38 (28) (2019) 5612–5626.

[18] L. Salmena, et al., A ceRNA hypothesis: the Rosetta Stone of a hidden RNA language? Cell 146 (3) (2011) 353–358.

[19] X. Guo, et al., Long non-coding RNA-HAGLR suppressed tumor growth of lung adenocarcinoma through epigenetically silencing E2F1, Exp. Cell Res. 382 (1) (2019), 111461.

[20] L. Jiang, et al., HCP5 is a SMAD3-responsive long non-coding RNA that promotes lung adenocarcinoma metastasis via miR-203/SNAI axis, Theranostics 9 (9) (2019) 2460–2474.

[21] Y. Cai, et al., LncRNA HMMR-AS1 promotes proliferation and metastasis of lung adenocarcinoma by regulating MiR-138/sirt6 axis, Aging (Albany NY) 11 (10) (2019) 3041–3054.

[22] Z. Ye, H. Jin, Q. Qian, Argonaute 2: a novel rising star in cancer research, J. Cancer 6 (9) (2015) 877–882.

[23] H. Wang, et al., STAT3-mediated upregulation of lncRNA HOXD-AS1 as a ceRNA facilitates liver cancer metastasis by regulating SOX4, Mol. Cancer 16 (1) (2017) 136.

[24] P.J. Batista, H.Y. Chang, Long noncoding RNAs: cellular address codes in development and disease, Cell 152 (6) (2013) 1298–1307.

[25] Y. Tay, J. Rinn, P.P. Pandolfi, The multilayered complexity of ceRNA crosstalk and competition, Nature 505 (7483) (2014) 344–352.

[26] C. Ye, et al., A novel long non-coding RNA lnc-GNAT1-1 is low expressed in colorectal cancer and acts as a tumor suppressor through regulating RKIP-NF-κB-Snail circuit, J. Exp. Clin. Cancer Res. 35 (1) (2016) 187.

[27] A. He, et al., Over-expression of long noncoding RNA BANCR inhibits malignant phenotypes of human bladder cancer, J. Exp. Clin. Cancer Res. 35 (1) (2016) 125.

[28] P. Malakar, et al., Long noncoding RNA MALAT1 promotes hepatocellular carcinoma development by SRSF1 upregulation and mTOR activation, Cancer Res. 77 (5) (2017) 1155–1167.

[29] M.M. Gottesman, et al., Toward a better understanding of the complexity of cancer drug resistance, Annu. Rev. Pharmacol. Toxicol. 56 (2016) 85–102.

[30] X.Z. Yang, et al., LINC01133 as ceRNA inhibits gastric cancer progression by sponging miR-106a-3p to regulate APC expression and the Wnt/β-catenin pathway, Mol. Cancer 17 (1) (2018) 126.

[31] M. Lv, et al., lncRNA H19 regulates epithelial-mesenchymal transition and metastasis of bladder cancer by miR-29b-3p as competing endogenous RNA, Biochim. Biophys. Acta Mol. Cell Res. 1864 (10) (2017) 1887–1899.

[32] X. Xue, et al., miR-342-3p suppresses cell proliferation and migration by targeting AGR2 in non-small cell lung cancer, Cancer Lett. 412 (2018) 170–178.

[33] D.H. Ma, et al., miR-93-5p/IFNAR1 axis promotes gastric cancer metastasis through activating the STAT3 signaling pathway, Cancer Lett. 408 (2017) 23–32.

[34] Y. Zhu, et al., MiR-17-5p enhances pancreatic cancer proliferation by altering cell cycle profiles via disruption of RBL2/E2F4-repressing complexes, Cancer Lett. 412 (2018) 59–68.

[35] B.S. Hong, et al., Tumor suppressor miRNA-204-5p regulates growth, metastasis, and immune microenvironment remodeling in breast cancer, Cancer Res. 79 (7) (2019) 1520–1534.

[36] T. Ye, et al., MicroRNA-7 as a potential therapeutic target for aberrant NF-κB-driven distant metastasis of gastric cancer, J. Exp. Clin. Cancer Res. 38 (1) (2019) 55.

[37] R. Liang, et al., SNHG6 functions as a competing endogenous RNA to regulate E2F7 expression by sponging miR-26a-5p in lung adenocarcinoma, Biomed. Pharmacother. 107 (2018) 1434–1446.

[38] Y. Jia, et al., LncRNA TTN-AS1 promotes migration, invasion, and epithelial mesenchymal transition of lung adenocarcinoma via sponging miR-142-5p to regulate CDK5, Cell Death Dis. 10 (8) (2019) 573.

[39] X. Zhao, et al., LncRNA HOXA11-AS drives cisplatin resistance of human LUAD cells via modulating miR-454-3p/Stat3, Cancer Sci. 109 (10) (2018) 3068–3079.

[40] J. Srivastava, J. DiGiovanni, Non-canonical Stat3 signaling in cancer, Mol. Carcinog. 55 (12) (2016) 1889–1898.

[41] Z. Liu, et al., STAT3-induced upregulation of long noncoding RNA HNF1A-AS1 promotes the progression of oral squamous cell carcinoma via activating Notch signaling pathway, Cancer Biol. Ther. 20 (4) (2019) 444–453.

[42] Y. Mo, et al., LINC01287/miR-298/STAT3 feedback loop regulates growth and the epithelial-to-mesenchymal transition phenotype in hepatocellular carcinoma cells, J. Exp. Clin. Cancer Res. 37 (1) (2018) 149.

[43] L. Yang, et al., Long noncoding RNA HEGBC promotes tumorigenesis and metastasis of gallbladder cancer via forming a positive feedback loop with IL-11/STAT3 signaling pathway, J. Exp. Clin. Cancer Res. 37 (1) (2018) 186.